# Shear and normal load perturbations on a two-dimensional continuous fault: 2. Dynamic triggering

H. Perfettini, J. Schmittbuhl, A. Cochard

# Shear and normal load perturbations on a two-dimensional continuous fault: 2. Dynamic triggering

H. Perfettini
Laboratoire de Géophysique Interne et Tectonophysique, Grenoble, France

J. Schmittbuhl
Laboratoire de Géologie, École Normale Supérieure, Paris, France

A. Cochard
Laboratoire de Détection et de Géophysique, Commissariat á l'Energie Atomique, Bruyères-le-Châtel, France
Laboratoire de Géologie, École Normale Supérieure, Paris, France

Received 31 January 2002; revised 28 August 2002; accepted 21 March 2003; published 3 September 2003.

[1] We study the consequences of temporal stress perturbations on earthquake nucleation in a continuous fault model. Using a two-dimensional (2-D) quasi-dynamic model of a strike-slip fault governed by a rate-and-state friction law with depth variable properties, we show that dynamic triggering (due to stress pulses or wave packets), although allowed by our results, is an exception rather than a rule and should be limited to understressed areas such as areas of high pore pressures or to faults at the very end of their earthquake cycle. When periodic stress perturbations are sensitive, the response of the fault is frequency-independent for periods lower than a period $T^0$ but strongly depends on the frequency for periods larger than $T^0$. We demonstrate that the crossover period $T^0$ is equal to the time left until the earthquake instability. According to our model, high frequencies are demonstrated to have a higher triggering potential than low ones, which makes tidal triggering very unlikely before the end of the cycle due to the very low amplitudes of the stress perturbations involved. *INDEX TERMS:* 7209 Seismology: Earthquake dynamics and mechanics; 7215 Seismology: Earthquake parameters; 7260 Seismology: Theory and modeling; *KEYWORDS:* earthquake triggering, dynamic triggering, Coulomb stress change, rate and state friction laws, clock advance/delay

**Citation:** Perfettini, H., J. Schmittbuhl, and A. Cochard, Shear and normal load perturbations on a two-dimensional continuous fault: 2. Dynamic triggering, *J. Geophys. Res.*, *108*(B9), 2409, doi:10.1029/2002JB001805, 2003.

## 1. Introduction

[2] Although the evolution of a fault is mainly controlled by its large scale tectonic environment, each fault strongly interacts with the local surrounding faults. In particular during the aftershocks sequence following a main shock, stress transfers strongly influence the future evolution of a seismic area. Indeed, the occurrence of an earthquake induces a change in the stress field surrounding the rupture plane. After a transient or dynamic change of stress induced by the passage of seismic waves, a static or permanent stress field is left around the ruptured fault. The companion paper by *Perfettini et al.* [2003] studies the influence of static variations in both the shear and/or normal stress on the triggering of an earthquake. Considering a two-dimensional (2-D) quasi-dynamic model of a continuous fault controlled by rate-and-state friction, we have shown that the predictions of the Coulomb failure model were reasonably close to the ones inferred using a more realistic fault model. In particular, the clock change (advance or delay) $\Delta t$ of an event roughly equals to $\Delta t = \Delta\mathrm{CFF}(\Delta\tau, \Delta\sigma)/\dot{\tau}$, where $\dot{\tau}$ is the tectonic stressing rate. Therefore the Coulomb stress change $\Delta\mathrm{CFF}(\Delta\tau, \Delta\sigma) = \Delta\tau - \mu_*\Delta\sigma$, where $\Delta\tau$ (respectively $\Delta\sigma$) is the shear (respectively normal) stress change on a fault of constant coefficient of friction $\mu_*$, appears as a useful tool for dealing with the static triggering of earthquakes. The fact that aftershocks seem to concentrate in areas of increased Coulomb stress (see *Harris* [1998] for a review) seems to confirm our results.

[3] The Coulomb failure model predicts that the effect of a transient change in the loading stress has no effect in terms of triggering unless these variations are large enough to bring the fault to the rupture threshold. However, many observations [e.g., *Gomberg and Bodin*, 1994; *Gomberg and Davis*, 1996; *Brodsky et al.*, 2000; *Gomberg et al.*, 2001] have suggested the existence of a dynamic triggering, i.e., some earthquakes may be triggered by the passage of seismic waves generated by a previous event, and this, even hundreds of kilometers away from the main shock. At a distance $R$ from


0148-0227/03/2002JB001805$09.00

the main shock, the static stress field decreases as $R^{-3}$ while the dynamic stress field due to body waves is decaying as $R^{-2}$. It follows that at great distances (typically $R > 100$ km) from the main shock, only the dynamic field is likely to trigger earthquakes, while static triggering should be more efficient closer to the hypocenter. We address in this paper the dynamic triggering. The study of static triggering has been discussed by *Perfettini et al.* [2003].

[4] We extend the work of *Gomberg et al.* [1998] by studying the effect of two types of transients: pulses and wave packets, in a 2-D continuous model. Moreover, perturbations of the loading stress include not only variations of the shear stress but also of the normal stress which allows an exact estimate of the Coulomb stress failure function.

[5] We assume that the temporal perturbations of the stress on the fault is due to the occurrence of a wave which arrives with a normal incidence. Doing so, the whole fault experiences the same stress variations with time. If the incidence of the wave is not normal, the wave of period $T$ induces spatial modulations of the stress field of wavelength $\lambda = cT$, where $c$ is the wave speed. Therefore it is impossible in that case, to decouple the effect of spatial and temporal variations of stress since both perturbations are linked due to the relation $\lambda = cT$. Here, we only focus on the response of the fault to temporal variations of the loading stress and neglect any spatial variations, which are beyond the scope of our paper.

## 2. Summary of the Modeling

[6] An extended description of the model is presented by *Perfettini et al.* [2003]. Here we introduce only a summary of the main aspects of the numerical model of the fault.

[7] In this study, we use a 2-D continuous quasi-dynamic fault model invariant along strike [see *Perfettini et al.*, 2003, Figure 1a]. The existence of a free surface is taken into account by considering a mirror image of the fault. The numerical domain of width $2L$ (the factor 2 arising from the presence of the mirror image) is divided into $n$ cells of length $\Delta x = 2L/n$ with $n = 256$, in order to properly describe the nucleation process. Slip, stress and velocity are computed in each individual cell. The friction on the fault is governed by rate-and-state friction [*Dieterich*, 1979; *Ruina*, 1983] and the frictional parameters are allowed to vary with depth. This model which accounts for the presence of the free surface is very similar to the model developed by *Rice* [1993]. In the rate-and-state framework, the frictional stress $\tau_i$ acting on the fault at cell $i$ is given by

$$\tau_i[V_i(t), \theta_i(t), \sigma_i(t)] = \sigma_i(t)\mu_i[V_i(t), \theta_i(t)], \tag{1}$$

where $\sigma_i(t) = \sigma_0 = 50$ MPa is the normal stress at point $i$ and is held constant at all depths (see *Perfettini et al.* [2003] for a justification). The coefficient of friction at point $i$ can be expressed as

$$\mu_i[V_i(t), \theta_i(t)]\mu_i^* + a_i \ln\left(V_i(t)/V_*\right) + b_i \ln\left(\theta_i(t)/\theta_*\right). \tag{2}$$

Therefore the evolution of friction at the $i$th cell requires the knowledge of the sliding velocity $V_i(t)$ and of the state variable $\theta_i(t)$. Two fundamental parameters appear in equation (2): $a_i$, and $b_i$. When $a_i > b_i$ then the slip on the cell tends to be stable and shows a velocity strengthening or creep behavior. When $a_i < b_i$, the cell presents a velocity weakening behavior and stick slip may be observed. In our model, the parameters $a$ and $b$ vary with depth as inferred by *Blanpied et al.* [1991] based on laboratory results. The shallow ($-2$ km $< z < 0$ km) and deep ($z < -15$ km) part of the fault are velocity strengthening regions showing a creep-like behavior, while at intermediate depths ($-15$ km $< z < -2$ km), the fault has a velocity weakening behavior [see *Perfettini et al.*, 2003, Figure 1b]. This last portion of the fault is the one where earthquakes nucleate and we refer to it as the seismogenic zone. The parameter $\mu_i^*$ is held constant at all depth, i.e., $\mu_i^* = \mu_* = 0.6$ as well as the constant reference velocity $V_*$ which was set to $V_* = 1$ μm/s.

[8] The evolution of the state variable with time at variable normal stress is given by [*Linker and Dieterich*, 1992]

$$\frac{d\theta_i(t)}{dt} = 1 - \frac{V_i(t), \theta_i(t)}{D_{c_i}} - \frac{\alpha_i\, \theta_i(t)}{b_i}\frac{\dot{\sigma}(t)}{\sigma(t)}, \tag{3}$$

where $\alpha_i = \alpha = 0.2$ at all depths. This value was derived from the laboratory measurements of *Linker and Dieterich* [1992] and *Richardson and Marone* [1999]. The characteristic length of evolution of friction is also constant at all depths and set to $D_c = 2$ cm. As discussed by *Perfettini et al.* [2003], this choice is dictated by numerical constraints but does not rely on observations since the value of $D_c$ is not yet constrained at the fault scale.

[9] The continuity of traction across the fault implies that

$$\tau_i[V_i(t), \theta_i(t), \sigma_i(t)] = \tau_i^0 - \frac{G}{2\beta}\left(V_i(t) - V_{pl}\right) + \Sigma_{j=1}^{n} K_{ij}\left(\delta_j(t) - V_{pl}\, t\right) + \Delta\tau_i(t), \tag{4}$$

where $\tau_i^0$ is the prestress on the fault, $G = 30$ GPa is the shear modulus, $V_{pl} = 35$ mm/yr is the plate velocity, while the kernel $K_{ij}$ is given by

$$K_{ij} = \frac{G}{2\pi\Delta x}\left[\frac{1}{(i-j)^2 - 1/4}\right] \tag{5}$$

and accounts for the static elastic interactions along the fault. Like in the work by *Stuart and Tullis* [1995], the derivation of equation (4) with respect to time yields, after the use of equation (3):

$$\begin{cases} \dot{V}_i(t) = \left[\Sigma_{j=1}^{n} K_{ij}\left(V_j - V_{pl}\right) - \left(\partial\tau_i/\partial\theta_i\right)\psi_i. \right. \\ \qquad\qquad \left. -\mu_i\,\dot{\sigma}_i + \Delta\dot{\tau}_i(t)\right] \Big/ \left[\partial\tau_i/\partial V_i + \dfrac{G}{2\beta}\right] \\ \dot{\theta}_i(t) = 1 - \dfrac{V_i(t), \theta_i(t)}{D_{c_i}} - \dfrac{\alpha_i\, \theta_i(t)}{b_i}\dfrac{\dot{\sigma}(t)}{\sigma(t)}. \end{cases} \tag{6}$$

The advantage of such rearrangement is that this system of $2n$ differential equations can be solved explicitly using a Runge-Kutta algorithm [*Press et al.*, 1992] with a fifth-order adaptative step-size control.

[10] With our choice of parameters, the fault rapidly enters a periodic regime, independent of the initial conditions, in which earthquakes occurs periodically with a recurrence or interseismic time of $T_{\mathbf{inter}} = 96.2$ years.

Perturbations are introduced at time $t_0$ after the last earthquake [see *Perfettini et al.*, 2003, Figure 2b]. They may alter the duration of the rest of the cycle, $t_p$, which, without perturbation, is denoted $t_f$ and is considered as a reference duration ($T_{\mathbf{inter}} = t_0 + t_f$). Clock advance or clock delay $\Delta t$ are estimates of the difference between the duration after perturbation, $t_p$, and the reference duration $t_f$: $\Delta t = t_f - t_p$. A clock advance corresponds to a positive $\Delta t$ and a clock delay to a negative $\Delta t$. The durations $t_f$ or $t_p$ are times to instability from the initiation time $t_0$. Instability is characterized as an increase of the maximum slip velocity on the fault above a prescribed threshold: $10^{-2}$ m/s (see *Perfettini et al.* [2003] for a justification of this value). Before considering the effect of shear and/or normal transient stress perturbations on the timing of an earthquakes, we define the Coulomb stress change as $\Delta\mathrm{CFF}(\Delta\tau, \Delta\sigma) = \Delta\tau - \mu_*\Delta\sigma$. As will be demonstrated in this paper, this quantity is, in most cases, particularly useful to account for simultaneous change in the shear and normal stress.

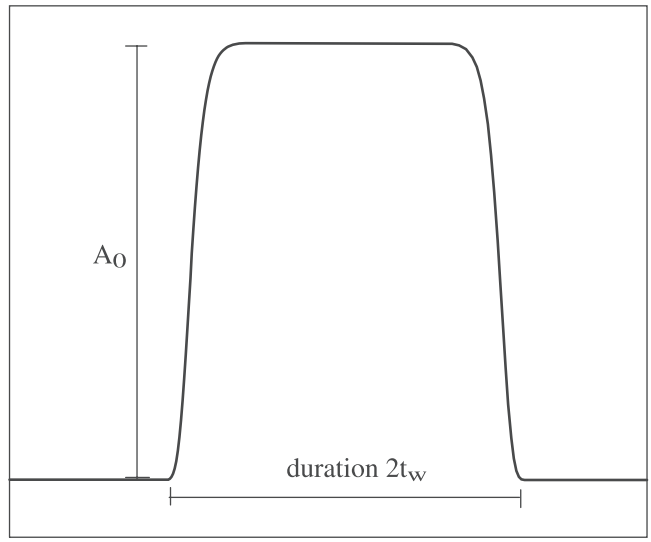


**Figure 1.** Pulse of amplitude $A_0$ and duration $2t_w$.

## 3. Stress Pulses

[11] We start our study by considering stress pulses. Even though no seismic waves generate such idealistic stress perturbations, they are of interest because of their simple shape, and because a real wave pattern results in a superposition of such pulses. Furthermore, as will be shown below, they allow the derivation of analytical expressions useful to predict the amplitude threshold for instantaneous triggering (see section 5).

[12] As in the work by *Gomberg et al.* [1997], we use pulses of the form

$$A(t) = A_0 \exp[-((t - t_0)/t_w)^n], \tag{7}$$

where $A(t)$ represents either normal or shear stress variations, $A_0$ is the maximum amplitude of the pulse, $t_0$ is the time at which the pulse reaches its maximum, and $t_w$ is the width or half duration of the pulse. The even integer $n$ modifies the risetime of the pulse: the bigger it is, the smaller the rise time. We decide to use $n = 16$, which corresponds to a very small risetime. Doing so, the pulse is very similar to a square wave, which is easier to use for analytical derivations. Such a pulse can be seen in Figure 1.

### 3.1. Influence of the Amplitude of the Pulse

[13] Figure 2 presents the clock advance due to stress pulses that promote failure (i.e., positive shear stress variations ($\Delta\mathrm{CFF}(\Delta\tau > 0,0)$) and negative normal variations ($\Delta\mathrm{CFF}(0, \Delta\sigma < 0)$)) as a function of their amplitude. The half duration of the pulse is fixed to $t_w = 500$ s while the time of application of the load is set to $t_0 = 94$ years. The clock advance has an upper limit $\Delta t = t_f - t_0$ (i.e., $t_p = t_0$) which is represented by the continuous line and corresponds to instantaneous triggering. We see that the clock advance is an increasing function of the amplitude.

[14] Shear and normal stress variations corresponding to a fixed Coulomb stress change $\Delta\mathrm{CFF}$ have qualitatively the same effect in terms of clock advance since the $\Delta\mathrm{CFF}(\Delta\tau, 0)$ (circles) and the $\Delta\mathrm{CFF}(0, \Delta\sigma)$ (triangles) curves are almost superimposed. This correspondence can be inferred looking at equation (6). We see that normal and shear stress variations contribute equally if $\Delta\tau_i = -\mu_i\Delta\sigma_i$, $i = 1, n$. The coefficient of friction $\mu_i$ varies during the earthquake cycle due to its dependence on sliding velocity, state variable and normal stress. However, it remains close to the constant value $\mu_*$ which is the dominant part of $\mu$, except during seismic rupture. Therefore it is reasonable to expect that a normal stress perturbation of amplitude $\Delta\sigma$ should have the same effect on the fault as a shear stress perturbation of amplitude $\Delta\tau \simeq -\mu_*\Delta\sigma$. We also found considering mixed perturbations in shear and normal stress, that all shear and normal combinations corresponding to a given Coulomb stress change $\Delta\mathrm{CFF}(\Delta\tau, \Delta\sigma)$, lead roughly to the same clock advance.

[15] The last observation that can be drawn out from examination of Figure 2 is that, except for small amplitudes (lower than 1 MPa), the clock advance $\Delta t$ and the amplitude $A$ of the pulse obey the scaling $A \propto \ln(\Delta t)$ which may also be expressed as $\Delta t \propto \exp(C\,A)$, where C is a positive constant. In the case of shear stress perturbation, we verified (see Figure 2) that the last scaling yields

$$\Delta t \propto \exp\left(\frac{\Delta\tau}{a\sigma_0}\right), \tag{8}$$

where $a = 0.015$ is the value of the $a$ parameter in the seismogenic zone. Equation (8) can also be obtained estimating $\Delta t$ using the analytical expression (B3) which gives the time to instability due to a square wave. Since any combinations in shear or normal stress resulting in the same Coulomb stress change lead to the same clock advance, equation (8) may more generally be expressed as $\Delta t \propto \exp(\Delta\mathrm{CFF}/a\sigma_0)$.

### 3.2. Influence of Duration $t_w$

[16] We study in this section the influence of the duration of the pulse on the clock advance. Figure 3 shows the clock advance as a function of the half duration $t_w$ of the pulses which are all applied at time $t_0 = 94$ years. Normal and shear stress perturbations were chosen in order to result in the same amplitude of the Coulomb stress

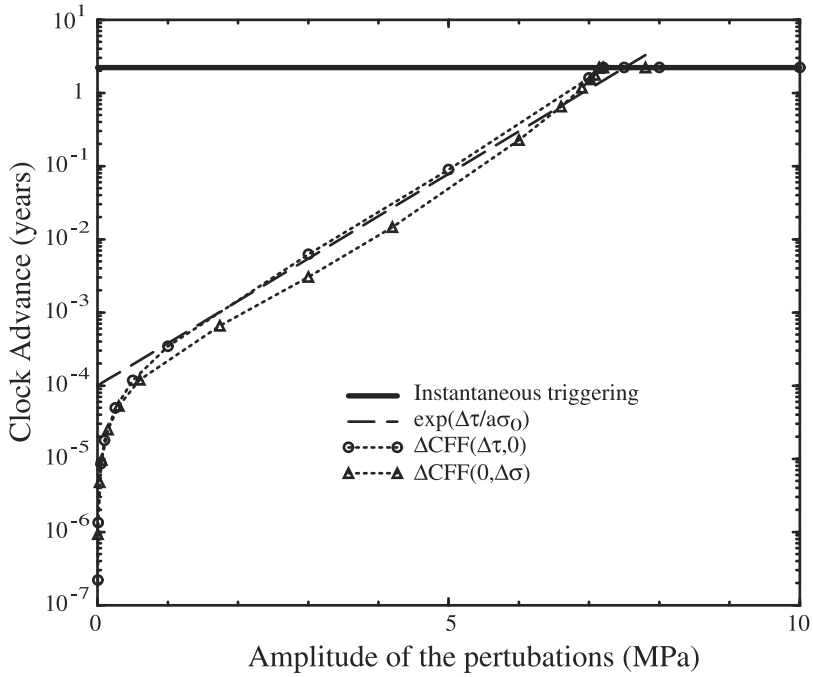


**Figure 2.** Clock advance (in years) as a function of the amplitude of the pulse. Pulses of normal stress (triangles) and shear stress (circles) are considered. The half duration of the pulse is $t_w$ = 500 s, and the pulse is applied at time $t_0$ = 94 years (for a 96.2-yearlong unperturbed cycle). Note that the clock advance due to a normal stress pulse of amplitude $\Delta\sigma$ is roughly equal to a pulse of shear stress of amplitude $\Delta\tau$ if $\Delta$CFF is constant (see triangles). The solid line corresponding to a clock advance of $\Delta t \simeq 2.2$ years represents instantaneous triggering.

change, i.e., $\Delta\mathrm{CFF}(\Delta\tau, 0) = \Delta\mathrm{CFF}(0, \Delta\sigma) = 6$ MPa. Such a Coulomb stress change is a large value but is needed in order to induce a noticable clock change. This illustrates the lack of efficiency of dynamic triggering due to its transient duration as will be discussed further in the text. The most important result is that the clock advance increases linearly with the duration of the pulse. As expected, the longer the duration of pulse, the greater the clock advance.

[17] This can also be checked analytically in the case of a shear stress pulse using the results of Appendix B. The clock advance $\Delta t = t_f - t_p$ can be obtained using equations (B1) and (B3), giving

$$\Delta t = \frac{-1}{\gamma} \ln\left[1 + \frac{2\exp(\gamma t_0)\sinh(\gamma t_w)(1 - \exp(\Delta\tau/(a\sigma)))}{1 + \frac{\gamma a}{H\dot{\delta}_0}}\right] \quad (9)$$

with $\gamma = \dot{\tau}/a\sigma_0$, $H = b/D_c - k/\sigma_0$, $\dot{\delta}_0$ being the initial mean velocity on the fault. As may be checked in Figure 3, the prediction of the analytical formula (9) is in qualitative agreement with the full numerical calculations.

[18] It is worth noting that since in Figure 3 the shear and normal stress pulses correspond to the same Coulomb stress change, one might naively have expected, in view of the static triggering results, to observe a comparable clock advance for both perturbations [see *Perfettini et al.*, 2003, Figure 8]. Their effect on clock advance, as mentioned by *Perfettini et al.* [2003], is all the more comparable when the actual friction coefficient remains close to $\mu_\star$. However, in the case of perturbations of limited duration, $t_w$, the characteristic time associated with $\alpha$ (defined in equation (3)) may become significant in front of $t_w$. We further discuss this issue in the next section.

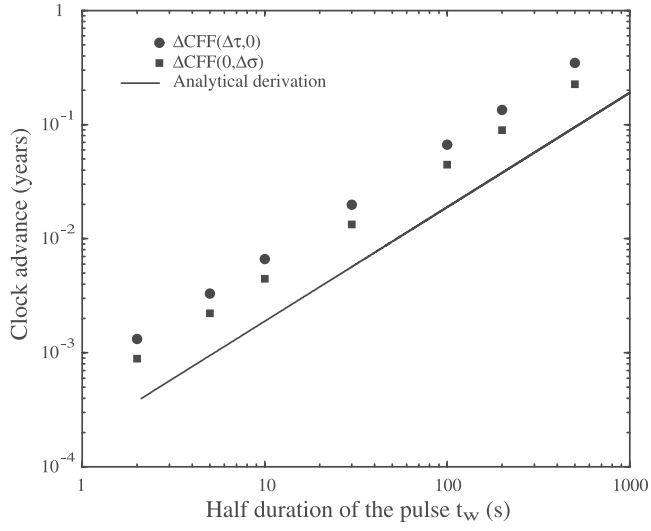


**Figure 3.** Influence of the duration of the pulse on the clock advance. Normal (circles) as well as shear (squares) stress pulses applied at time $t_0$ = 94 years are considered. The clock advance increases linearly with the duration of the pulse. An analytical expression (see text) for the clock advance due to a shear stress (square) pulses is in rough agreement with the full numerical calculations.

### 3.3. Loading Versus Unloading Pulses

[19] We have studied so far the effect of loading pulses ($\Delta$CFF > 0), i.e., pulses that promote failure. It is worth looking at unloading pulses, that is, pulses that inhibit the occurrence of the earthquake. Figure 4 shows the clock change as a function of the amplitude of the pulses applied at time $t_0 = 94$ years and of fixed duration $t_w = 200$ s. Solid and open symbols correspond respectively to unloading and loading pulses. Shear stress pulse (circles) as well as normal stress pulses with $\alpha = 0.2$ (squares) and $\alpha = 0$ (diamonds) are considered. The effect of the parameter $\alpha$ is to diminish the effect of normal stress perturbations: the larger $\alpha$, the lower the effect of the normal stress change on the sliding surface. The existence of such a parameter has been demonstrated experimentally by *Linker and Dieterich* [1992] for bare rock surfaces and confirmed by *Richardson and Marone* [1999] considering a gouge layer. We see from Figure 4 that unloading and loading pulses have similar effects for low magnitude. However, they do not have an equivalent influence on the fault for large magnitudes. Unloading pulses of large magnitude induce a much lower clock change than similar loading pulses. For instance, an unloading normal stress pulse of amplitude $\Delta\sigma = 10$ MPa leads to a clock delay of $-\Delta t \simeq 0.01$ years while a loading normal stress pulse of amplitude $\Delta\sigma = 10$ MPa creates a clock advance of $\Delta t = 0.46$ years. However, the difference between loading and unloading pulses fails even for large magnitudes if the sensitivity to normal stress perturbation is increased: $\alpha = 0.2$.

[20] Let us propose a qualitative explanation of the observed behaviors. As discussed in the previous section, for a given value of $\Delta$CFF, the different effects on, say, clock change, of various combinations of $\Delta\sigma$ and $\Delta\tau$ are comparable if the actual friction coefficient remains close to $\mu_\star$. For $\alpha = 0$ or for shear-only stress perturbations, the second term, $-V\theta/D_c$, on the right-hand side in equation (3) is negative. The actual coefficient $\mu$ will thus "naturally" drift from $\mu_\star$. We now suppose non zero normal load perturbations and $\alpha \neq 0$. For unloading pulses, the third term $-\alpha\theta\dot{\sigma}/(b_i\sigma)$ in equation (3) is negative (since $\dot{\sigma} > 0$ for unloading pulses). Accordingly, its contribution is the same as that of the previous term, resulting in enhancement of the drift. By contrast, for loading pulses, the contribution is opposite to the natural drift; hence the criterion $\Delta$CFF = const is better fulfilled, in agreement with what is observed in Figure 4.

## 4. Wave Packet

[21] The power spectrum of a seismic wave is more complex since not only one period is represented. To simplify the problem and to study the frequency effect of the wave on the timing of the instability, we propose, as done by *Gomberg et al.* [1997], to model a seismic train of amplitude $A(t)$ by the following function:

$$A(t) = A_0 \sin\left(\frac{2\pi t}{T}\right) \exp\{-[(t - t_0)/t_w]^n\}, \qquad (10)$$

where $A_0$ is the maximum amplitude of the pulse, $T$ the period of the wave, $t_0$ the time for which the wave amplitude reaches its maximum value, $t_w$ the half width of the wave pattern, and $n = 16$ an integer that controls the risetime. Such a virtual seismogram consists of a pulse like envelope inside which oscillations at period $T$ occur (see Figure 5).

[22] In order to examine the period effect of the wave, we estimated the clock advance due to the presence of a wave train of infinite duration. The reason for this choice is that, perturbation periods are not limited by $t_w$ for wave train of infinite duration. We will study the effect of the duration further in the text but as expected, the longer the wave train, the larger the clock advance.

### 4.1. Influence of the Period

[23] We look at the clock advance due to a wave train of infinite duration and of period $T$. The amplitude $A(t)$ of this wave is given by:

$$A(t) = A_0\, R(t) \sin\left(\frac{2\pi t}{T}\right), \qquad (11)$$

where $R(t)$ is a ramp function, i.e., $R(t) = 0$ for $t < 0$, $R(t) = 1$ for $t > t_1$, and $R(t) = (1 + \sin[\pi(t - t_1/2)/(t_1)]/2$ for $0 < t < t_1$. The risetime $t_1$ is set to $t_1 = 100$ s and is considered in order to apply the load not too abruptly.

[24] The response of the fault to periodic variations of the loading stress is complex and depends on the amplitude and frequency of the oscillations in a non trivial manner. This is illustrated in Figure 6 which shows the relative clock advance $\Delta t/t_f$ as a function of the period of the perturbation applied at time $t_0 = 94$ years. Various Coulomb stress changes are considered: $\Delta$CFF($\Delta\tau$, 0) = 1 and 5 MPa, and $\Delta$CFF(0, $\Delta\sigma$) = 1 and 5 MPa. The numerical results are compared to analytical derivations obtained using the formalism of Appendix A. To estimate these analytical forms that are obtained by considering a 1-D model, the initial velocity on the fault is needed and we use the mean velocity around the nucleation point (located at 5 km depth) which is of the order of $\dot{\delta}_0 = 5.5\ 10^{-10}$ m/s at that time in the earthquake cycle. The semianalytical derivations capture the behavior of the relative clock advance as a function of the period of the perturbations.

[25] A crucial point can be made looking at Figure 6, which shows that the fault response to normal stress perturbations is different from the response to shear stress variations even when the Coulomb stress change induced by these fluctuations is the same. Normal stress fluctuations lead to a lower clock advance than shear stress ones due to the effect of the unloading part of the load variation. Such a feature has been previously noticed and has been discussed in section 3.3 (Figure 4) when unloading pulses were considered.

### 4.2. A Crossover Period $T^0$

[26] Figure 6 shows a plateau at low periods and a complex structure at higher periods. The period $T^0$ for which the transition between these two regimes occurs has been derived analytically in Appendix B3 and leads to

$$T^0 = \frac{2\pi a}{\dot{\delta}_0 H g(\Delta\tau)} \qquad (12)$$

with $H = b/D_c - k/\sigma_0$, $k$ being the equivalent stiffness of the fault. The function $g$ is given by

$$g(\Delta\tau) = \int_0^{2\pi} \exp[\Delta\tau \sin(y)/(a\sigma_0)]dy, \qquad (13)$$

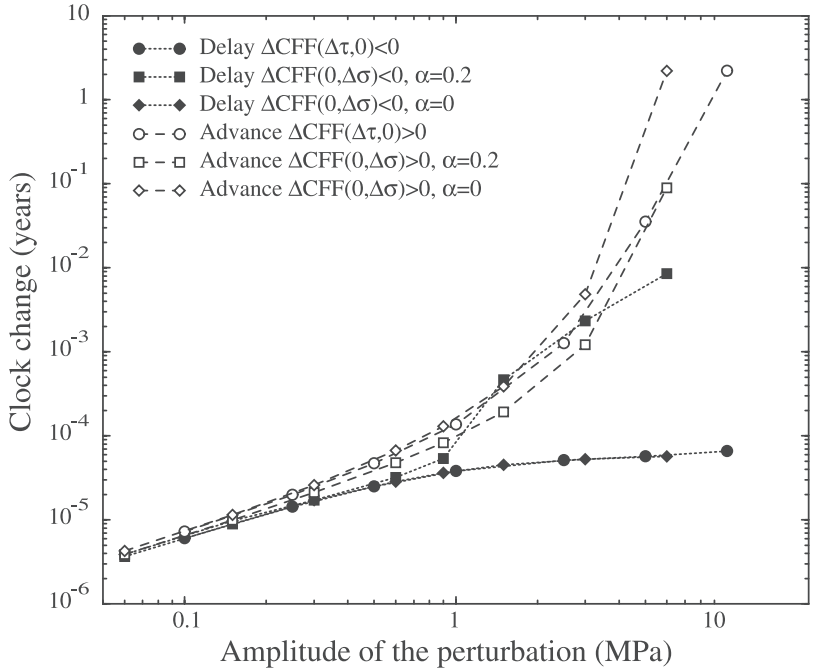


**Figure 4.** Clock delay due to unloading pulses (solid symbols) ($\Delta\tau < 0$ or $\Delta\sigma > 0$) applied at time $t_0$ = 94 yrs and of half duration $t_w$ = 200 s. The influence of the normal stress is studied changing the $\alpha$ parameter: $\alpha = 0.2$ (squares) and $\alpha = 0$ (diamonds). For the sake of comparison, the clock advance (open symbols) due to a shear stress step ($\Delta\tau > 0$) and to normal stress pulses ($\Delta\sigma < 0$) with $\alpha = 0.2$ and $\alpha = 0$ is also shown. Note that the clock delay becomes negligible compared to the clock advance at high amplitudes (typically greater than $a\sigma_0$).

which can be estimated numerically. Since in the seismogenic zone $b/D_c \simeq 0.95$ m$^{-1}$ and $k/\sigma_0 \simeq 0.03$ m$^{-1}$, we find that $H \simeq b/D_c$, yielding:

$$T^0 \simeq \frac{2\pi a D_c}{\dot{\delta}_0 b g(\Delta\tau)}. \quad (14)$$

At low periods ($T \to 0$) the time to instability $t_p(T \to 0)$ is frequency-independent and is given by (see Appendix B3)

$$t_p(T \to 0) = T^0 = \frac{2\pi a}{\dot{\delta}_0 H g(\Delta\tau)}. \quad (15)$$

Accordingly, $T^0 = t_p(T \to 0)$ which means that the transition period between the non sensitive and the sensitive domain is nothing else than the time to instability. Using equation (12), we found that $T^0 \simeq 1.9\ 10^7$ s for $\Delta\tau = 1$ MPa, while $T^0 \simeq 2.2\ 10^5$ s for $\Delta\tau = 5$ MPa, both values being in agreement with Figure 6. It is important to note that $T^0 = t_p(T \to 0)$ means that the response of the fault is changing radically when the period of the perturbations reaches the time to the next earthquake. Such a feature has been observed by *Beeler and Lockner* [2003], who measured experimentally the frictional response of a fault to periodic variations of the loading stress and, in particular, the degree of correlation between the occurrence of the simulated earthquakes and permanent oscillations of the external load. They found that above a given period $t_n = 2\pi a\sigma_0/\dot{\tau}$, the microearthquakes were correlated with the stress perturbations, if the perturbation was of significant amplitude. Unlike the transition period $t_n$ of *Beeler and Lockner* [2003], the period $T^0$ in our model given in equation (14) depends on the time where the perturbation starts (through the initial velocity $\dot{\delta}_0$ which varies throughout the earthquake cycle), the ratio $a/b$, the characteristic length $D_c$, and the amplitude $\Delta\tau$ which appears in equation (13) via the $\Delta\tau/a\sigma_0$ term. We believe that one major cause of the difference between $t_n$ and $T^0$ comes from the fact that the stress perturbations in the experiment of *Beeler and Lockner* [2003] are permanent (in order to simulate Earth tides) and may therefore, modify the properties of the earthquake cycle, e.g., its duration.

[27] The existence of the transition period $T^0$ can also be observed in Figure 7 which shows the relative clock advance

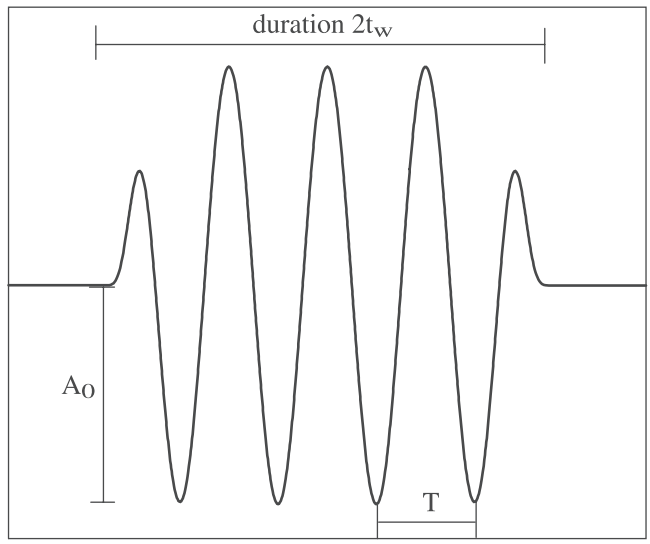


**Figure 5.** Wave packet of amplitude $A_0$, duration $2t_w$ and period $T$.

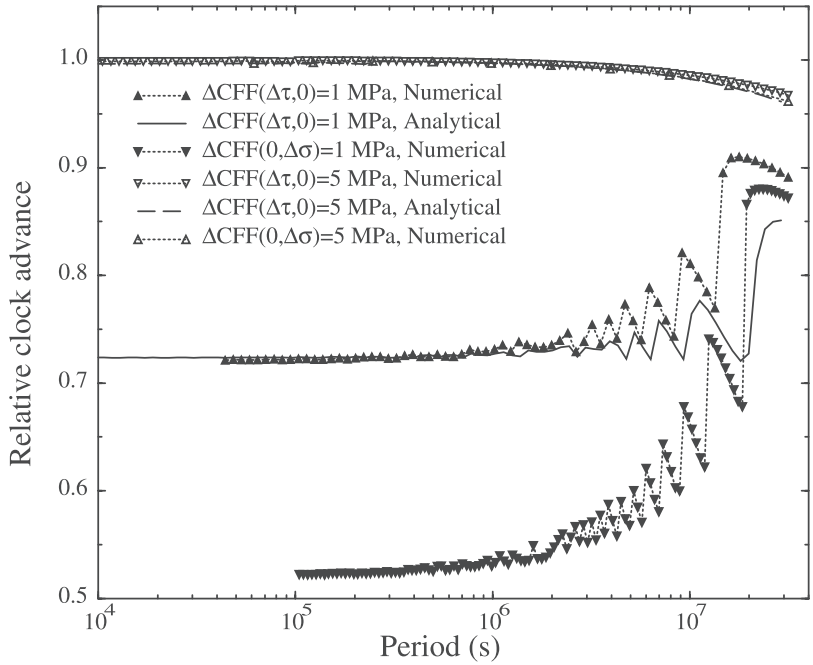


**Figure 6.** Relative clock advance $\Delta t/t_f$ as a function of the period of the perturbation applied at time $t_0$ = 94 years and considering a wave train of infinite duration. Numerical results corresponding to Coulomb stress changes of amplitude $\Delta CFF(\Delta\tau, 0)$ = 1 MPa, $\Delta CFF(\Delta\tau,0)$ = 5 MPa, and of amplitude $\Delta CFF(0, \Delta\sigma)$ = 1 MPa are compared to semianalytical derivations which requires the knowledge of the initial sliding velocity on the fault. Note that the semianalytical derivations capture the behavior of the full numerical calculations.

due to shear stress perturbations $\Delta\tau(t) = \Delta\tau \sin(2\pi t/T)$ of amplitude $\Delta\tau$ = 1 MPa as a function of the period of the wave train, and considering various initial sliding velocities $\dot{\delta}_0 = 10^{-2}$, $10^{-4}$, $10^{-6}$, and $10^{-8}$ m/s. The period $T$ is normalized by the transition period $T^0$ given in equation (12). The clock advance was derived using the semianalytical formalism of Appendix A (see equation (A1)) to reduce significantly the computational time and explore a larger parameter space. After normalization of the period by $T^0$, all the curves collapse in Figure 7, which illustrates the $1/\dot{\delta}_0$ dependence of the crossover period $T^0$ predicted by equation (12). The transition period $T^0$ which is also equal to the time left before the occurrence of the earthquake defines the limit period between two regimes: For $T < T^0$ the response of the fault is period-independent because the number of oscillations experienced by the fault before the instability is extremely large. When the period $T$ reaches $T^0$, the period of the perturbation becomes important as can be seen in Figure 7. For very large periods of the perturbations ($T \gg T^0$) the clock advance tends to zero independently of the period. Indeed, in that case, the earthquake occurs before any significant change in the loading stress has occurred. In other words, the rate of variation of the shear stress is very small compared to the loading rate $\dot{\tau}$ (i.e., $\omega\Delta\tau \gg \dot{\tau}$) and the fault becomes insensitive to the stress variations.

[28] The change in the fault behavior for $T \gtrsim T^0$ makes the fault highly sensitive to the envelope of the stress perturbation, a dependence which vanishes for $T < T^0$. To illustrate that point, we have computed the relative clock advance due to shear stress perturbations of the type $\Delta\tau(t) = \Delta\tau \sin(2\pi t/T)$ for various initial velocities and a shear stress amplitude $\Delta\tau = -1$ MPa (see Figure 7). Therefore the shear stress perturbation is initially decreasing with time instead of increasing. The results are shown in Figure 7 where again, the period is normalized by the crossover period $T^0$. For $T < T^0$, the clock advance is constant and equal to $\Delta t/t_f \simeq 0.3$, as in the case $\Delta\tau$ = 1 MPa. This illustrates again the frequency independence of the load for low periods ($T < T^0$). When $T \gg T^0$ the clock advance tends to 0 as in the $\Delta\tau$ = 1 MPa case. In the intermediate regime $T \gtrsim T^0$, the fault is sensitive to the envelope of the shear stress variations which are, in the case $\Delta\tau = -1$ MPa, unloading the fault. This is illustrated by a negative clock advance.

[29] The results shown in Figure 7 allow us to give a new physical meaning to the transition period $T^0$. It is the period above which the fault response becomes dependent on the exact form of the perturbation applied. This interpretation is consistent with the definition of *Beeler and Lockner* [2003], who define $T^0$ as the period above which their experimentally simulated earthquake correlate with the external load fluctuations. It is also important to note that the clock advance at low periods ($T \ll T^0$) is much larger than at high periods ($T \gg T^0$) for which the clock change tends to 0. Therefore high frequencies have a higher triggering potential than low frequencies in agreement with the seismological observation of *Gomberg and Davis* [1996] and the theoretical work of *Roy and Marone* [1996].

### 4.3. Influence of the Phase Lag

[30] Perturbations of magnitude $\Delta CFF(\Delta\tau, 0)$ = 1 MPa and $\Delta CFF(\Delta\tau, 0) = -1$ MPa differ only by their phase lag. Accordingly, the influence of the phase lag is illustrated in Figure 7. For very low periods, the clock advance is significant but independent of the phase lag. At high

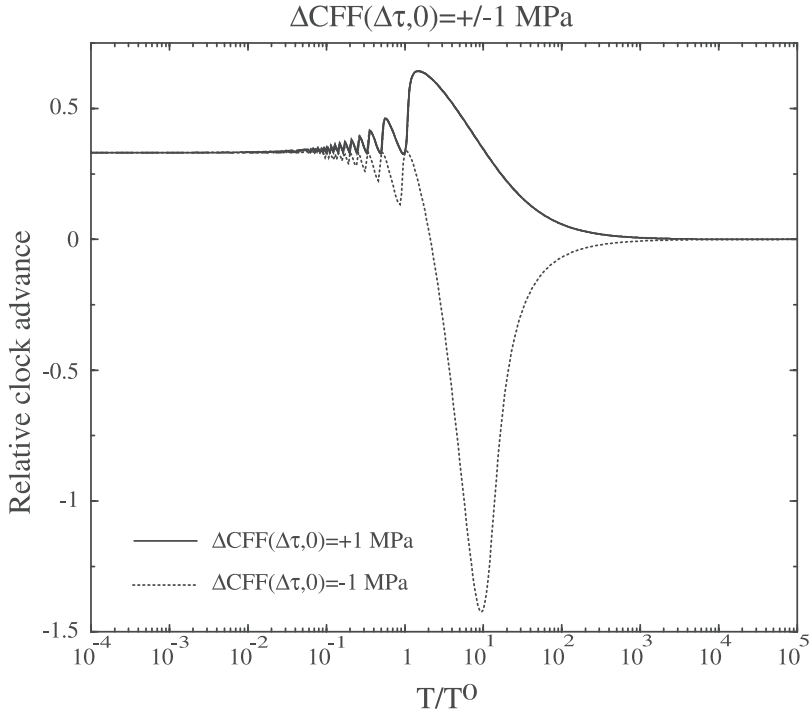


**Figure 7.** Relative clock advance $\Delta t/t_f$ as a function of the period of the perturbation assuming a wave train of infinite duration of amplitude $\Delta CFF(\Delta\tau, 0) = 1$ MPa (thick lines) and $\Delta CFF(\Delta\tau, 0) = -1$ MPa (thin lines). The period $T$ is normalized by the transition period $T^0$ given in equation (12). The analytical formalism of Appendix A (see equation (A1)) has been used. Various initial sliding velocities namely $\dot{\delta}_0 = 10^{-2}$, $10^{-4}$, $10^{-6}$, and $10^{-8}$ m/s are considered, corresponding to various time in the earthquake cycle (the higher the sliding velocity, the later the time in the earthquake cycle). After normalization of the period by $T^0$, all the curves for a given perturbation magnitude, perfectly superimposed, illustrating the $1/\dot{\delta}_0$ dependence of the crossover period $T^0$. This figure illustrates the two regimes of the fault response. At low periods, the response of the fault is frequency-independent but becomes highly sensitive to the frequency of the load variations at higher periods (before becoming independent again at very high periods, when there is effectively no perturbation at all).

periods, there is no clock change of the fault. However, for periods close to $T^0$, the phase lag has a strong influence: the fault can be very significantly advanced or close to locked.

[31] However, the phase lag of the arriving wave train is controlled by the focal mechanism of the remote earthquake. Even if we consider in our model only normal incidences of the wave train, we clearly see that there is a major difference in the fault response according to the properties of the remote earthquake. Two remote earthquakes with a similar source function but different orientations of the focal planes, located in the same region at a given distance of the fault might either enhance or inhibit the fault. There is a strong directivity effect. Moreover, we see from Figure 7 that the phase lag induces "nonsymmetrical" effects. The maximal clock advance from a perturbation of magnitude $\Delta CFF(\Delta\tau, 0) = 1$ MPa is more than two times smaller than the maximal clock delay induced by a perturbation of magnitude $\Delta CFF(\Delta\tau, 0) = -1$ MPa. This "nonsymmetric" influence has also been observed for static loading or unloading steps [see *Perfettini et al.*, 2003].

### 4.4. Influence of the Amplitude

[32] We now look at the influence of the amplitude of the shear stress perturbations on the clock advance of rupture. Figure 8 presents the relative clock advance $\Delta t/t_f$ for a shear stress perturbation $\Delta\tau(t) = \Delta\tau \sin(2\pi t/T)$ for various amplitudes $\Delta\tau = 0.1$, 1, 2.5, 5, 10 MPa. The initial velocity is $\delta_0 = 10^{-2}$ m/s (we use in this section the semianalytical formula based on the formalism of Appendix A (see equation (A1)) and for which time to instability has been defined as the time for which the sliding velocity becomes infinite) and is characteristic of faults at the very end of the earthquake cycle. Also displayed on Figure 8 is the clock advance at the transition period (diamonds) given in equation (12) and corresponding to the amplitudes considered. The locations of the predicted crossover periods successfully separate the frequency-independent with the frequency-dependent regime. The main observation from Figure 8 is that the transition period $T^0$ decreases with increasing amplitude, and tends to zero at large amplitudes. The clock advance is also increasing with increasing $\Delta\tau$, but this feature is also due to the choice $\Delta\tau > 0$. Considering $\Delta\tau < 0$ would have led to an opposite conclusion for $T > T^0$ since the perturbation starts by unloading the fault.

### 4.5. Influence of the Duration

[33] We now look at the influence of the duration of the wave train on the clock advance. Figure 9 shows the clock advance as a function of the half duration $t_w$ of a wave packet of normal stress amplitude $\Delta\sigma = -10$ MPa applied

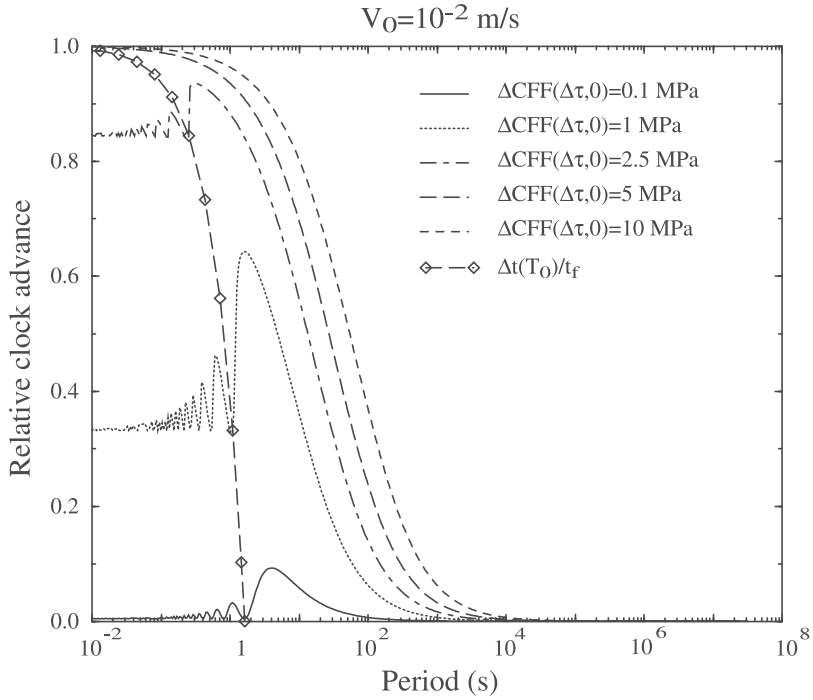


**Figure 8.** Relative clock advance $\Delta t/t_f$ as a function of the period of the perturbation considering a wave train of infinite duration applied on a fault of initial sliding velocity $V_0 = 10^{-2}$ m/s, i.e., a fault at the end of its earthquake cycle. Various shear stress amplitudes are considered: $\Delta\tau = 0.1$ MPa, $\Delta\tau = 1$ MPa, $\Delta\tau = 2.5$ MPa, $\Delta\tau = 5$ MPa, $\Delta\tau = 10$ MPa. The relative clock advance at the transition period is also displayed (diamonds) and separates the two regimes of the fault response.

at time $t_0 = 94$ years. The period of the wave train was set to $T = 10$ s. As in the case of the pulse, the clock advance is increasing linearly with the duration of the pulse. Again the longer the perturbation is applied, the bigger its effect.

### 4.6. Comparison Between Pulses and Wave Packets

[34] *Gomberg et al.* [1998] proposed that the effect of a wave packet and a squares wave were qualitatively equal in terms of triggering as long as their duration, width and amplitude were similar. We can discuss this statement in the light of our results. For periods lower than $T^0$, we expect the detailed shape of the perturbing signal not to be so important, due to the frequency independence at low periods. However, at long periods, namely greater than $T^0$, we showed that the frictional response of the fault was highly dependent on the frequency of the perturbing stress. In this case, considering a square wave or a sine wave makes a significant difference. Therefore we believe that before simplifying the stress variations to a square wave, one should verify that the maximum period of the wave train does not exceed $T^0$.

## 5. Instantaneous Triggering

[35] In this section, we examine the minimum amplitude for instantaneous triggering. As will discussed in the next two sections, our definition of instantaneous triggering is rather arbitrary but choosing other definitions will lead to the same qualitative conclusions.

### 5.1. Pulses

[36] When considering the effect of pulses in our model, triggering is said to be instantaneous if it occurs during the passage of the pulse (i.e., in the time interval $[t_0 - t_w; t_0 + t_w]$). We define the onset of triggering when the maximum velocity on the fault exceeds $10^{-2}$ m/s.

[37] The minimum amplitude noted $A^c$ (where $A^c = \Delta\mathrm{CFF}(\Delta\tau, 0)$ for shear stress perturbations and $A^c = \Delta\mathrm{CFF}(0, \Delta\sigma)$ for normal stress perturbations) for instanta-

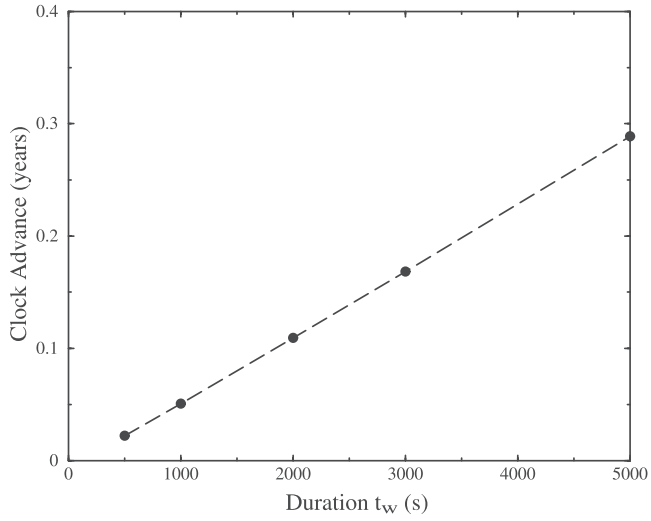


**Figure 9.** Clock advance as a function of the half duration $t_w$ of a wave packet of normal stress amplitude $\Delta\sigma = -10$ MPa applied at time $t_0 = 94$ years. The period of the wave is $T = 10$ s.

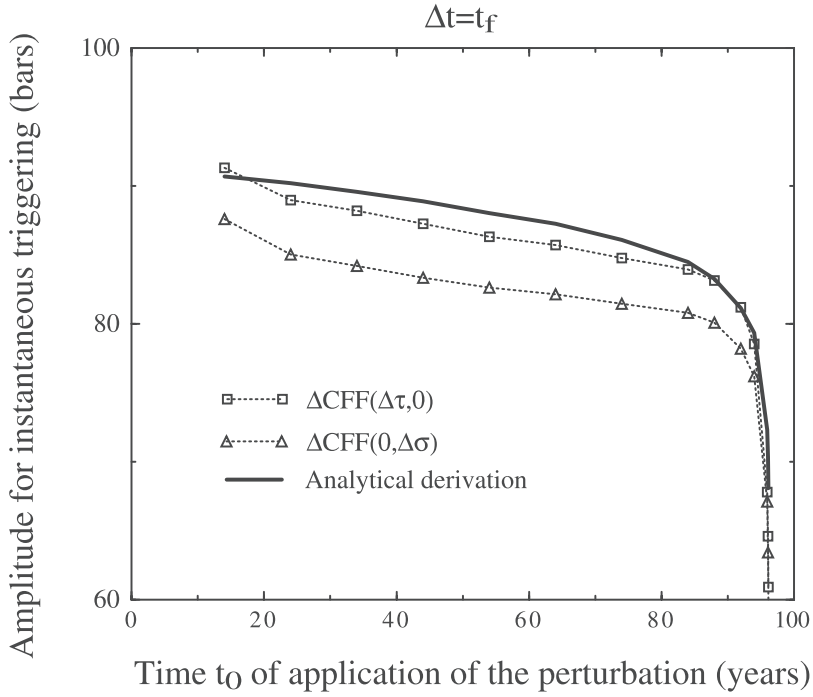


**Figure 10.** Minimum amplitude for instantaneous triggering as a function of the time $t_0$ of application of the pulse. All the pulses have a half duration of $t_w$ = 200 s. At the instantaneous triggering threshold, normal stress pulses (circles) and shear stress pulses (squares) of same maximum Coulomb stress change ΔCFF, have roughly the same triggering potential. An analytical derivation is in good agreement with the numerical results.

neous triggering is shown in Figure 10 as a function of the time of application of the stress perturbation $t_0$. The half width of the pulse is held constant with $t_w$ = 200 s.

[38] The most important feature is that the threshold amplitude $A^c$ is decreasing with increasing $t_0$. This is due to two features. First, the clock advance is equal to $\Delta t = t_f - t_0$ and is linearly decreasing with the time of application of the load $t_0$. Therefore a smaller amplitude is needed for instantaneous triggering the later the load is applied. Ultimately, at the very end of the cycle, instantaneous triggering is related to a clock advance $\Delta t = t_f - t_0$ that tends to 0 since $t_0 \rightarrow t_f$. In this case, the least perturbation can bring the fault to failure. The second feature is that the later the transient load is applied, the bigger the clock advance. This comes from the fact that the slip variation due to the effect of a transient variation of the loading stress on the fault is bigger at the end of the earthquake cycle rather than at the beginning because the sliding velocities involved are much higher. Therefore, for a given duration of the pulse, the clock change is significantly larger at the end than at the beginning of the earthquake cycle.

[39] As noticed previously in the paper, normal and shear stress variations have the same qualitative effect when $\Delta\tau \simeq -\mu_* \Delta\sigma$, or in other words, when they result in the same Coulomb stress change $\Delta CFF(\Delta\tau, \Delta\sigma)$.

[40] We have been able in Appendix B2 to give an analytical estimate of the amplitude for instantaneous triggering considering shear stress pulses only. This approximation was obtained considering the 1-D equivalent model, i.e., a spring block model and is in good agreement with the numerical results (see Figure 10). The minimum amplitude $\Delta\tau^c$ for instantaneous triggering is given by:

$$\Delta\tau^c = a\sigma_0 \ln\left[1 + \frac{a\gamma}{\dot{\delta}_0 H} \frac{\exp(-\gamma t_0)}{2\sinh(\gamma t_w)}\right], \qquad (16)$$

where the parameters are defined in Appendix B2. The equivalent stiffness of the fault has been taken as $k = (2/\pi) G/L$ [see *Perfettini et al.*, 2003], where $L$ = 20 km is the size of the fault. The frictional parameters $a$ and $b$ for the spring slider model are equal to their value in the seismogenic zone of our 2-D model, i.e., $a$ = 0.015 and $b$ = 0.019. The normal stress is $\sigma_0$ = 50 MPa and the characteristic length of the friction law is $D_c$ = 2 cm. The initial velocity $\dot{\delta}_0$ in the spring slider model was obtained taking the initial velocity $\delta_0$ around the nucleation point in our 2-D model. Equation (16) also contains the parameter $\gamma = \dot{\tau}/(a\sigma_0)$, where the loading stress rate $\dot{\tau}$ verifies $\dot{\tau} = k V_{pl}$.

[41] As discussed in Appendix B2, one can get rid of the initial velocity $\dot{\delta}_0$ by replacing it by the time to failure $t_f$ in the absence of perturbations given by equation (B1).

### 5.2. Wave Packet of Infinite Duration

[42] The minimum amplitude $\Delta\tau^c$ for instantaneous triggering as a function of the frequency of a shear wave $\Delta\tau(t) = |\Delta\tau| \sin(2\pi t/T)$ is presented in Figure 11 and was computed using the semianalytical approximation given in Appendix B (see equation (B6)). This type of perturbation promotes rupture at low frequencies. As discussed in section 4.2, this will not be the case for a shear stress change of the form

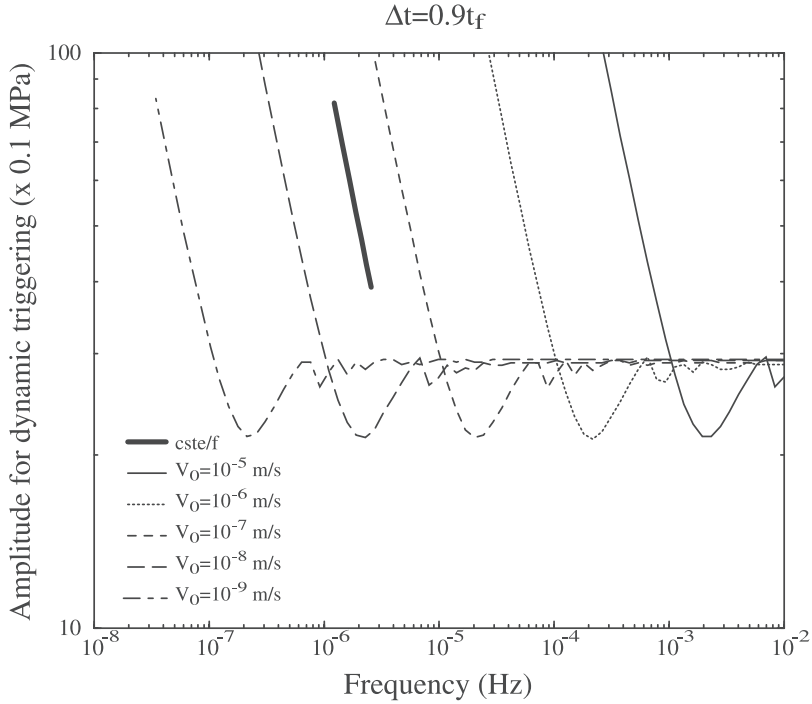


**Figure 11.** Minimum shear stress amplitude as a function of the frequency of the wave packet in order for the wave train of infinite duration to clock advance the instability by 90%. Again, the fault response shows two regimes: regime I, a frequency-independent regime at high frequencies and regime II, a frequency-dependent regime where the threshold amplitude scales as $1/f$.

$\Delta\tau(t) = -|\Delta\tau| \sin(2\pi t/T)$, since at low frequencies ($T \gg T^0$), such perturbations unload the fault.

[43] The stress perturbation of infinite duration was applied considering various initial sliding velocities namely $\dot{\delta}_0 = 10^{-5} - 10^{-9}$ m/s and therefore corresponds to different times in the earthquake cycle. Instantaneous triggering was determined at a given frequency, by increasing the amplitude until the relative clock advance exceeds 90%. This definition is arbitrary but taking for instance a relative clock advance of 99% leads qualitatively to the same results.

[44] Figure 11 shows that the fault response may be divided in two regimes. At high frequencies, instantaneous triggering occurs for an amplitude of $\Delta\tau \simeq 3$ MPa, a threshold which is frequency-independent. At low frequencies, the amplitude threshold $\Delta\tau^c$ scales as $\Delta\tau^c \propto 1/f$. The period for which this transition occurs depends on the initial sliding velocities, in agreement with equation (12) and the comments of section 4.2.

[45] Such a $1/f$ scaling has already been proposed by *Lockner and Beeler* [1999]. They studied, using granite samples, when the occurrence of their laboratory simulated earthquakes was correlated with an externally periodic perturbation of the loading stress. For a given frequency, they have been able to approximately determine the shear stress amplitude over which correlation occurs. The correlation plot they have made [see, e.g., *Lockner and Beeler*, 1999, Figure 8] is very similar to our Figure 11, i.e., it exhibits a $1/f$ behavior as $f \to 0$, and a plateau for $f \to \infty$. Our results are therefore in agreement with the work of *Lockner and Beeler* [1999].

[46] Considering the triggered seismicity in The Geysers due to the Landers seismic waves, *Gomberg and Davis* [1996] found that the strain threshold function $\epsilon_T(f)$ for dynamic triggering was

$$\epsilon_T(f) \simeq \frac{0.1}{f}\ \mu\text{strain}, \tag{17}$$

which again, shows a $1/f$ scaling. Equation (17), which was obtained considering frequencies in the range $10^{-3}$ – 10 Hz, implies that for an antiplane problem, the shear stress threshold is of the order of $\Delta\tau^c(f) \simeq 2G\epsilon_T(f)$, where $G$ is the shear modulus. The fact that *Gomberg and Davis* [1996] observe a frequency dependence of the strain spectrum suggest that $1/T^0$ is lower than the maximum frequency considered by these authors, i.e., $1/T^0 > 10$ Hz or $T^0 < 0.1$ s When instantaneous triggering is considered, the transition period is difficult to estimate using equation (12) since this formula contains the amplitude of the perturbation which we are looking for. However, a rough estimate can be given noting that in the expression of the $g$ function of (13), the amplitude only shows up through the $\Delta\tau/a\sigma_0$ term. Therefore an estimate can be obtained taking $\Delta\tau = a\sigma_0$. This leads to $T^0 \simeq 2\pi a/\dot{\delta}_0 H g(a\sigma_0)$. One can verify that with the parameters of the model (given by *Perfettini et al.* [2003, sections 3 and 4]), the inequality $k/\sigma_0 \ll b/D_c$ holds. Since $H \simeq b/D_c$ and that usually $a \simeq b$ [*Marone*, 1998], and noting that $g(a\sigma_0)$ is of the order of unity leads to $T^0 \simeq D_c/\dot{\delta}_0$. We find that one must have $\dot{\delta}_0 = 10^{-5}$ m/s for $D_c = 1$ μm (lower bound for laboratory values) and $\dot{\delta}_0 = 0.1$ m/s for $D_c = 10$ cm (upper bound given by seismological observations), in order to meet the requirement $T^0 = 0.1$ s. A sliding velocity of the order of $10^{-5}$ m/s is significant in our model and is only obtained at the very end of the earthquake cycle. We suggest

that the faults considered by *Gomberg and Davis* [1996] and triggered by the seismic waves of the Landers sequence were rather close to failure at the arrival of the wave train.

### 5.3. Wave Packet of Finite Duration

[47] In this section, we consider the minimum amplitude for instantaneous triggering considering wave packets of finite half duration $t_w$ = 500 s applied at various times $t_0$ of the earthquake cycle. As mentioned previously, the use of a finite duration limits the upper period to be considered to $T = t_w$.

[48] Figure 12 presents the amplitude threshold for instantaneous triggering considering wave packets of period $T$ = 5 s (pluses), $T$ = 50 s (squares), and $T$ = 500 s (circles) as a function of the time $t_0$ when they are applied. Figure 12 is qualitatively similar to Figure 10 derived for pulses (note that the duration of the perturbation is different between the two cases). The first observation that can be made is that the amplitude for instantaneous triggering is decreasing with increasing time of application of the load $t_0$ showing again that for transient stress perturbations, the later the load is applied the bigger its effect. We recall that this results from the fact that the later the perturbation, the closer the fault is to the velocity threshold corresponding to the onset of instability.

[49] Finally, the minimum amplitude for dynamic triggering is constant at low periods (the $T$ = 5 s and $T$ = 50 s curves are alike). At higher periods, namely, the case $T$ = 500 s of Figure 12, the amplitude $\Delta\tau^c$ is bigger than at low periods. This is consistent with the fact that high frequencies have a higher triggering potential than low ones but also that this effect saturates at very low periods as illustrated by the similarity between the $T$ = 5 and 50 s curves in Figure 12 or the plateau as $T \rightarrow 0$ in Figures 6–8.

## 6. Discussion: Comparison With Existing Observations

### 6.1. Dynamic Triggering (DT)

[50] Dynamic triggering has been recently considered as a candidate for earthquake triggering. It is important to note that DT seems to be an exception rather than a rule since only very few studies have reported a positive effect. DT due to the passage of the seismic waves generated by the Landers earthquake are mentioned by *Gomberg and Bodin* [1994] for the case of the $M$ = 5.4 Little Skull Mountain event, *Anderson et al.* [1994] for the Western Great Basin, while *Gomberg and Davis* [1996] mention some triggered seismicity in The Geysers geothermal field. In all these studies, surface waves seem to be responsible for the triggering but a crucial remark is that most of the areas where DT have been reported following the Landers sequence involve magmatic, volcanic or more generally geothermal areas where high fluid pressure is expected. We will discuss this point later in the section.

[51] Another case of DT concerns the Irpinia earthquake sequence. *Belardinelli et al.* [1999] computed the dynamic stress field generated by the rupture of the first segment of the 1980 ($M_s$ = 6.9) Irpinia earthquake at the location of the second subevent which was separated by a time interval of 20 s. The authors estimated, using an analytical expression of the clock advance due to a step of shear stress (with $\Delta\tau \simeq$ 1.5 MPa) in the absence of tectonic loading, that the parameter $a\sigma_0$ has to be of the order of $a\sigma_0 \simeq 0.08$ MPa to explain the 20-s-long delay between the two subevents, a value of the same order as the previous estimate of *Toda et al.* [1998] ($a\sigma_0 \simeq 0.035$ MPa). Using the analytical formula given in (B4) with $a$ = 0.006, $t_w \simeq$ 5 s, $a\sigma_0$ = 0.035 MPa, the parameters estimates of *Belardinelli et al.* [1999], we find that the minimum amplitude for instantaneous triggering is ofÂthe order of 1.2 MPa for an initial sliding velocity of $\dot{\delta}_0 = 10^{-10}$ m/s and of the order of 0.04 MPa for $\dot{\delta}_0 = 10^{-3}$ m/s. These two values are below the peak value of $\Delta\tau$ = 1.5 MPa mentioned by Belardinelli et al. Therefore our results are consistent with an explanation of this sequence in terms of dynamic triggering.

[52] At remote distances from the hypocenter, the wave train arriving on the fault is long, the wave pattern being composed of body waves and surface waves. The dynamic stress field roughly decays as $1/R^2$ for body waves and as $1/R^{3/2}$ for surface waves, where $R$ is the distance between the observation point and the earthquake hypocenter. Therefore, in terms of the amplitude of the perturbations, surface waves have a higher triggering potential than body waves. In addition to this, the duration of the wave train of surface waves is much longer than for body waves, meaning than stress perturbations due to surface waves are applied longer than in the case body waves. Our results seem to favor high frequency waves for dynamic triggering although examination of Figure 12 shows that the triggering "potential" is roughly constant for periods lower than $T^0$. Because of the $1/\dot{\delta}_0$ scaling of $T^0$, this frequency independence is less pronounced for faults at the very end of the earthquake cycle since $T^0 \rightarrow 0$ as $\dot{\delta}_0 \rightarrow \infty$. Despite the fact that our model predicts that high frequencies are more destabilizing than low ones, we expect surface waves to be much more efficient for dynamic triggering than body waves. The main reasons for this is that surface waves have a much higher amplitude and a longer duration, both factors being fundamental for DT as we showed previously.

[53] Assuming a wave train of infinite duration, we showed in Figure 11 that the triggering threshold was of the order of 3 MPa for the periods involved in the dynamic wave pattern. This is twice bigger than the value reported in the literature, i.e., $\Delta\tau$ = 1.5 MPa for the Irpinia sequence [*Belardinelli et al.*, 1999], and of the order of $\Delta\tau \simeq 0.1$ MPa for the Landers sequence [*Gomberg and Bodin*, 1994; *Anderson et al.*, 1994; *Gomberg and Davis*, 1996]. Our results show that DT is easier if (1) the fault is at the end of the earthquake cycle since the amplitude threshold for instantaneous triggering drops to zero when the stress perturbation is applied at the very end of the earthquake cycle and (2) the normal stress on the fault is very low. Indeed and as showed by the analytical result given in equation (B4) obtained for a pulse, the amplitude for instantaneous triggering scales as $a\sigma_0$. This scaling can be easily inferred by the following reasoning. When a perturbation is suddenly applied, it results in a variation of the sliding velocity. If $V^+(t)$ is the sliding velocity immediately after the shear stress variation and $V^-(t)$ its value before, then [see *Perfettini et al.*, 2003, equation (B6)]

$$\frac{V^+(t)}{V^-(t)} \simeq \exp[\Delta\tau/(a\sigma_0)]. \tag{18}$$

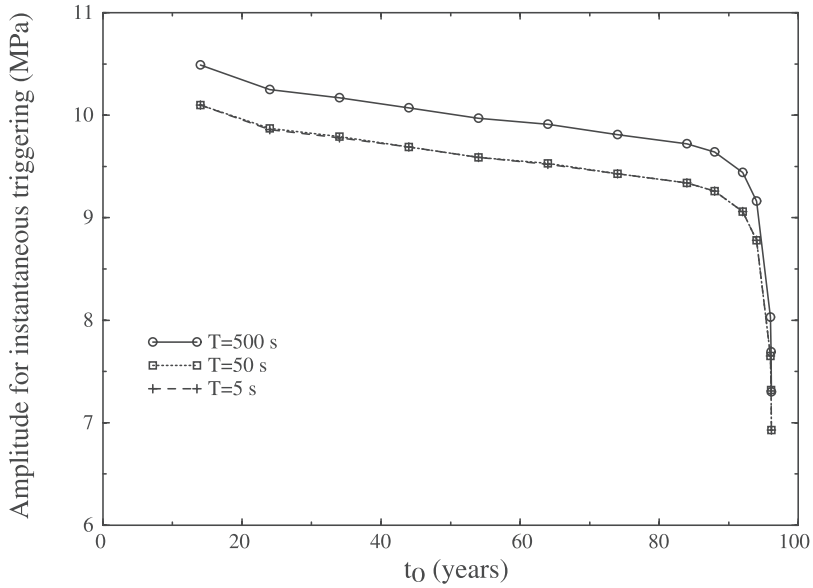


**Figure 12.** Minimum amplitude for instantaneous triggering as a function of the time $t_0$ of application of a wave packet of shear stress. All the wave trains have a half duration of $t_w$ = 500 s. Wave packets of period $T$ = 5, 50 and 500 s are considered. The triggering threshold for the low periods $T$ = 5, 50 s are similar while it is higher for the long-period case $T$ = 500 s showing that low periods have a higher triggering potential than high periods.

Equation (18) shows the importance of the parameter $p = \Delta\tau/(a\sigma_0)$. When $p \gg 1$, there is a sudden increase in the slip velocity due to the perturbation which can result in instantaneous triggering, while for $p \ll 1$, the viscous effect arising from the existence of the $a$ term in equation (2) reduces the effect of the instability. One way of making DT to occur for lower triggering amplitudes is to reduce the normal stress. If the normal stress on the fault is reduced from $\sigma_0$ to $\sigma_0$/const, where Const. is a constant greater than 1, then the amplitude for instantaneous triggering drops from $\Delta\tau_c$ to $\Delta\tau_c$/Const.. In our modeling, the value of $a\sigma_0$ in the seismogenic zone is of the order of $a\sigma_0$ = 0.75 MPa, a value which seems one order of magnitude bigger than the estimates of *Toda et al.* [1998] or *Belardinelli et al.* [1999]. This suggests either that the normal stress on these faults is one order of magnitude lower than what we proposed or that the parameter $a$ is much smaller than what we suggested. Since in most studies [*Marone*, 1998], $a$ is of the order of $10^{-2}$, we believe that a normal stress reduction is more likely to be responsible for the DT reported. This remark is in agreement with the fact that most of the areas where DT has been reported following the Landers earthquake involves geothermal areas where the effective normal stress on the fault is expected to be low. An increase of seismicity in a geothermal area has also been reported in the Yalova cluster following the Izmit earthquake (H. Perfettini et al., Dynamic triggering following the Izmit earthquake, submitted to *Geophysical Research Letters*, 2002).

[54] To end this section, we refer to an example of late dynamic triggering [*Brodsky et al.*, 2000] reported DT in Greece due to the surface waves of the 1999 Izmit earthquake. As noticed by these authors, the region of triggered seismicity is a nonvolcanic area and no geothermal activity is expected. *Brodsky et al.* [2000] propose that this DT case could be explained by the faults being in a near-critical state, which, in our model, would correspond to a fault close to failure. Therefore this case is also consistent with our results.

### 6.2. Particular Case of Tidal Triggering

[55] Earth tides result from the gravitational attraction of the sun and the moon and create periodic variations of the stress acting on a fault of amplitude of the order of 0.001 to 0.004 MPa [*Vidale et al.*, 1998]. Most of the existing studies on this process have answer negatively to the existence of tidal triggering. *Vidale et al.* [1998] discussed tidal triggering by resolving the normal, shear and Coulomb stress on earthquake fault planes of their catalog made of a large number of events (13,042 earthquakes). They found a weak (2%) correlation which was not considered as significant. Recent experimental work by *Lockner and Beeler* [1999] confirm this conclusion. A correlation between the occurrence of laboratory simulated earthquakes and a periodic variations of the loading stress was only observed for amplitudes at least two orders of magnitudes larger than tidal triggering amplitudes. These observations are in agreement with our results. Indeed, looking at Figure 11, we see that the minimum amplitude for dynamic triggering with an infinite wave train is of the order of 3 MPa. This result is not in favor of tidal triggering because of the large amplitudes involved. However, at the very end of the earthquake cycle, namely when the time to failure $t_f$ is approaching the period $T$ of the wave train, the effect of the wave train is reduced to the effect of a pulse. Accordingly, instantaneous triggering is likely for very small stress perturbations. Therefore we expect tidal triggering to be possibly efficient at the very last stage of the earthquake cycle.

[56] Measuring the phase lag between earthquakes occurrence and tidal loading peaks, *Tsuruoka et al.* [1995] considered a global catalog of 998 earthquakes with magnitude greater than 6. They observed no correlation for strike-

slip and thrust-type earthquakes occurrence but a correlation was noticed for normal-fault type earthquakes. This observation is very difficult to reconcile with our results or the previous works mentioned earlier. However, it has to be mentioned that *Perfettini and Schmittbuhl* [2001] showed that the measure of the phase lag was not a good tool to detect tidal triggering due to the non linearities off the friction law we use.

## 7. Conclusions

[57] Using a 2-D continuous fault model with depth variable frictional properties, we have studied the triggering effect of dynamic stress changes in shear as well as in normal stress. A first study had been carried on by *Gomberg et al.* [1998], who studied the effect of transient stress changes in terms of clock advance. However, that study was based on a spring slider model hence implicitly with uniform frictional properties and considered shear stress variations only.

[58] First of all, our results show that the spring slider model seems to be adapted for such studies, as illustrated by the agreement between the analytical derivations and the full numerical results. This also suggests that the shallow and deep part of the fault, which have a velocity strengthening behavior and which do not exist in a 1-D model such as a spring block system, do not affect qualitatively the fault behavior. Creeping at a constant velocity $V_{pl}$ during most of the earthquake cycle, they increase the loading stress on the velocity weakening (or seismogenic zone), shortening the duration of the earthquake cycle. Therefore the spring block model is a rather satisfying fault model in the quasi-dynamic approximation but its range of validity remains limited since it is unable to account for spatial heterogeneities and can thus only model an homogeneous fault.

[59] An important result of this study is that normal and shear stress variations have roughly (except for unloading pulses, see Figure 4) the same triggering potential if they lead to the same Coulomb stress change $\Delta CFF(\Delta\tau, \Delta\sigma) = \Delta\tau - \mu_*\Delta\sigma$, in which the coefficient of friction is $\mu_*$ is constant and represents the static and dominant part of the coefficient of friction given in equation (2). Therefore estimating the Coulomb stress changes is particularly useful to account for simultaneous fluctuations in the shear and normal stress. However, there are at least two circumstances for which normal and shear stress perturbations of same Coulomb stress change do not lead to the same clock advance. The first of them is when the perturbation is applied at the very end of the earthquake cycle when the coefficient of friction begins to differ significantly from the value $\mu_*$ that we have used as the reference coefficient of friction [see *Perfettini et al.*, 2003]. The second circumstance is when the transient perturbation are of very small periods and/or duration. In that case, the presence of the $\alpha$ term in equation (3) and which characterizes the instantaneous response of the fault to normal stress variations, induces important differences between normal and shear transient perturbations.

[60] We also showed that dynamic triggering by seismic waves, although allowed by our model, is rather unlikely. Indeed, it can only occur for faults under low normal stresses, for instance due to high fluids pore pressure, and/or for faults at the very end of the seismic cycle. We showed that an amplitude threshold for instantaneous dynamic triggering exists but depends on the time at which the perturbations is applied as illustrated by equation (B4) in the case of shear stress pulses.

[61] Before ending this discussion, we want to insist on the fact that in our model, the whole fault experiences the same stress variations, which corresponds, in the dynamic case, to a seismic wave arriving with normal incidence. If the incidence of the wave is not normal, the wave of period $T$ induces spatial modulations of the stress field of wavelength $\lambda = cT$, where $c$ is the wave speed. Owing to the concept of nucleation size $L_c$ [*Dieterich*, 1992; *Rice*, 1993], wavelengths with $\lambda > L_c$ are unstable while the modes related to $\lambda < L_c$ are stable. This means that when spatial modulations of stress are considered, long wavelengths have a higher destabilizing effect than short ones. This is illustrated in the results of *Voisin* [2001], who found, using a linear slip weakening law, that long wavelengths or periods where fastening the duration of the nucleation phase. Ignoring spatial stress modulations, we reached an opposite conclusion; that is, high frequencies have a higher triggering potential. It is difficult to know whether or not short of long periods are more able to trigger earthquakes since in general stress variations occur both in time and space. However, the laboratory results of *Lockner and Beeler* [1999] and the data analysis of *Gomberg and Davis* [1996] both suggest that short periods are more efficient to trigger earthquakes than long ones. Therefore we believe that our conclusions regarding the frequency effect on triggering should be extended to the case of a dynamic wave arriving with an oblique incidence.

## Appendix A: General Comments on the Time to Instability $t_p$

[62] *Perfettini et al.* [2003] demonstrate that the time to instability $t_p$ in the presence of shear stress perturbations $\Delta\tau(t)$ can be obtained by solving

$$F(t_p) = \frac{a}{H} \tag{A1}$$

with

$$F(t) = \dot{\delta}_0 \int_0^t [1 + C(y)]^{-b/a} \exp[(\dot{\tau} y + \Delta\tau(y))/(a\,\sigma_0)]dy, \tag{A2}$$

where $H = (b/D_c) - (k/\sigma_0)$. We recall that in the rest of this appendix that $\gamma = \dot{\tau}/(a\sigma_0)$, this parameter being the inverse of the aftershock duration $t_a = a\sigma_0/\dot{\tau}$ defined by *Dieterich* [1994].

[63] Let $\epsilon$ be the maximum amplitude of the shear stress perturbations. Introducing $\gamma = \dot{\tau}/(a\sigma_0)$ and $\beta = \epsilon/(a\sigma_0)$, equation (A2) becomes:

$$F(t) = \dot{\delta}_0 \int_0^t [1 + C(y)]^{-b/a} \exp[\gamma y + \beta\, g(y)]dy, \tag{A3}$$

where the function $g$ incorporates all the time dependence of the shear stress perturbations. Deriving equations (A3) with respect to the parameters $\gamma$ and $\beta$, we find

$$\frac{\partial F}{\partial \gamma} = \dot{\delta}_0 \int_0^t y\,[1 + C(y)]^{-b/a} \exp[\gamma y + \beta\, g(y)]dy \tag{A4}$$

$$\frac{\partial F}{\partial \beta} = \dot{\delta}_0 \int_0^t g(y)\,[1 + C(y)]^{-b/a} \exp[\gamma y + \beta\, g(y)]dy. \tag{A5}$$

Since $y > 0$, equation (A4) implies that $\partial F/\partial\gamma > 0$. Following the comments of *Perfettini et al.* [2003, Appendix C], we find that $\partial t_p/\partial\gamma < 0$. Recalling that $\gamma = \dot{\tau}/(a\sigma_0)$, we find that (1) the time to instability is decreasing with increasing stress rate $\dot{\tau}$, and (2) the time to instability is increasing with increasing parameter $a$ or mean normal stress $\sigma_0$.

[64] The dependence of the time to instability $t_p$ with the parameter $\beta$ is not so trivial since it depends on the function $g$. However, if $g(y)$ is apositive function ($g(y) > 0$ for all $y$), then $\partial t_p/\partial\beta > 0$. In this case, the time to instability verifies $\partial t_p/\partial\gamma < 0$. For a transient positive variation of the shear stress, the time to instability is decreasing with increasing amplitude of the perturbation. The opposite conclusion is reached when a negative transient is considered. The case of an oscillating signal such as $g(u) = \sin(\omega u)$ is more complicated.

[65] Previous analytical works [*Dieterich*, 1992; *Gomberg et al.*, 1998] used the approximation $C(y) = 0$ to reach the same conclusions. However, as noticed by these authors, such an approximation was only valid at the end of the earthquake cycle where $V\theta/D_c \gg 1$. Our work uses equation (A2) which is the exact solution of the state variable evolution law. Therefore the conclusions of *Dieterich* [1992] or *Gomberg et al.* [1998] can be extended to any time of the earthquake cycle. It is crucial to note that our conclusions are based on a very simple fault model, i.e., the spring block model should not be extended to a real fault without extreme cautious.

## Appendix B: Applications

### B1. Case of No Stress Perturbations

[66] The time to instability $t_f$ in absence of shear stress perturbations was estimated by *Perfettini et al.* [2003], yielding

$$t_f = \frac{a\sigma_0}{\dot{\tau}} \ln\left[1 + \dot{\tau}/\left(\sigma_0 H \dot{\delta}_0\right)\right]. \tag{B1}$$

### B2. Case of a Stress Pulse

[67] We consider a shear square wave of half duration $t_w$ applied at time $t_0 - t_w$: $\Delta\tau(t) = \Delta\tau\,[H(t - t_0 + t_w) - H(t - t_0 - t_w)]$, where $H(t)$is the Heaviside function. Let us first calculate the function $F(t)$ given by equation (A2) assuming $C(y) \ll 1$, an assumption that is valid for a fault late in the earthquake cycle (see the end of Appendix A). Using equation (A2), we find

$$F(t) = \frac{\dot{\delta}_0}{\gamma}\{\exp(\gamma t) - 1 - 2\exp(\gamma t_0)\sinh(\gamma t_w) \cdot[1 - \exp(\Delta\tau/(a\sigma_0))]\}, \tag{B2}$$

where $\gamma = \dot{\tau}/(a\sigma_0)$. The time to instability $t_p$ verifies $F(t_p) = a/H$ and is therefore given by

$$t_p = \frac{1}{\gamma}\ln\left[1 + \frac{a\gamma}{\dot{\delta}_0 H} + 2\exp(\gamma t_0)\sinh(\gamma t_w)[1 - \exp(\Delta\tau/(a\sigma_0))]\right]. \tag{B3}$$

Using equation (B3), we can derive an expression for the minimum amplitude for instantaneous triggering. Noting that equation (B3) is decreasing with increasing amplitude $\Delta\tau$, the time to instability reaches its minimum value when the argument of the logarithm reaches 1 (and not 0 in order for the time to instability to remain positive). Let us call $\Delta\tau^c$ the amplitude of the shear stress pulse for which it happens. Using equation (B3), it is easy to find

$$\Delta\tau^c = a\sigma_0 \ln\left[1 + \frac{a\gamma}{\dot{\delta}_0 H}\frac{\exp(-\gamma t_0)}{2\sinh(\gamma t_w)}\right]. \tag{B4}$$

Therefore, knowing the initial velocity, it is possible to estimate the minimum amplitude for instantaneous triggering. If the initial velocity is unknown but the time to instability $t_f$ without any perturbations is know, one can use equation (B1) to replace the constant $\frac{a\gamma}{\dot{\delta}_0 H}$ in B4 by $\exp(\gamma t_f) - 1$. In this case, equation (B4) can also be written as

$$\Delta\tau^c = a\sigma_0 \ln\left[1 + \left(\exp\left(\gamma t_f\right) - 1\right)\frac{\exp(-\gamma t_0)}{2\sinh(\gamma t_w)}\right]. \tag{B5}$$

Even though equation (B5) looks rather complicated, it maybe used to qualitatively estimates if instantaneous triggering is expected. Imagine that the interseismic time $T_{\text{inter}}$ is approximately known (because of historical records or paleoseismological data). If no major surrounding earthquakes have struck the area since the last major event on the fault, then one can assume that the time left before instability at time $t_0$ verifies $t_f = T_{\text{inter}} - t_0$. If at time $t_0$ a train wave of half duration $t_w$ and of maximum amplitude $\Delta\tau$ hits the fault, then it may be useful to compare $\Delta\tau$ with $\Delta\tau^c$ given in equation (B5). If $\Delta\tau \gg \Delta\tau^c$ then instantaneous triggering is expected, while the train wave should not have much affected the fault dynamic if $\Delta\tau \ll \Delta\tau^c$.

### B3. Case of Periodic Variations of the Loading Stress

[68] Let us consider the effect of a wave train of infinite duration such as $\Delta\tau(t) = \Delta\tau\, f(\omega t)$, where $f(t)$ is a periodic function of period $2\pi$. The function $F(t)$ in equation (A2) can be written in the case where $C(y) \ll 1$:

$$F(t) = \dot{\delta}_0 \int_0^t \exp[\gamma y + \Delta\tau f(\omega y)/(a\sigma 0)]dy \tag{B6}$$

or alternatively, after the change of variable $y \to \omega y$:

$$F(t) = \frac{\dot{\delta}_0}{\omega}\int_0^{\omega t} \exp[\gamma y/\omega + \Delta\tau f(y)/(a\sigma 0)]dy. \tag{B7}$$

[69] At low periods ($\omega \to \infty$) the integral of equation (B7) becomes

$$F(t) \simeq \frac{\dot{\delta}_0}{\omega}\int_0^{\omega t} \exp[\Delta\tau f(y)/(a\sigma 0)]dy. \tag{B8}$$

Let us write when $T \to 0$, $n = \text{int}(t/T)$, where int(..) means integer part, $n \gg 1$ being an integer. The function $F(t)$ reads in this case

$$F(t) \simeq \frac{\dot{\delta}_0}{\omega}\, n\, g(\Delta\tau) \tag{B9}$$

with

$$g(\Delta\tau) = \int_0^{2\pi} \exp[\Delta\tau f(y)/(a\sigma 0)]dy, \tag{B10}$$

where implicitly, we have neglected in the expression of $F(t)$ a term which cannot exceed $g(\Delta\tau)$. This is justified if $n \gg 1$. Remembering that $n \simeq t/T$, equation (B9) becomes

$$F(t) \simeq \frac{t\dot{\delta}_0 g(\Delta\tau)}{2\pi}. \quad \text{(B11)}$$

The time to instability $t_p(T \to 0)$ is obtained writing $F(t_p) = a/H$ giving

$$t_p(T \to 0) = \frac{2\pi a}{\dot{\delta}_0 H g(\Delta\tau)}. \quad \text{(B12)}$$

Equation (B12) gives the time to instability when extremely low periods are considered. This time is not depending on the frequency of the perturbations.

[70] The period $T^0 = 2\pi/\omega^0$ above which the period dependence starts may be roughly estimated writing $\omega^0 t_p(T \to 0) \simeq 2\pi$. This corresponds to the case where the upper limit of the integral (B7) corresponds to one period of oscillation. This leads to $T_0 = t_p(T \to 0)$ so that

$$T^0 = \frac{2\pi a}{\dot{\delta}_0 H g(\Delta\tau)}. \quad \text{(B13)}$$

The fact that $T_0 = t_p(T \to 0)$ means that the transition period between high and low frequencies is equal to the time to instability, i.e., the time left before the earthquake. Therefore the period $T_0$ varies throughout the earthquake cycle, decreasing with increasing time. At the very end of the cycle $\left(\dot{\delta}_0 \to \infty\right)$, $T_0$ is near 0 meaning that the fault response strongly depends on the frequency of the stress perturbations.

[71] **Acknowledgments.** A special thanks to J. R. Rice, who originally motivated this work. We are grateful to C. Marone and S. Nielsen for their thoughtful review and suggestions. We are very grateful to M. Bouchon and R. Archuleta for numerous discussions. Thanks to A.-M. Boullier, who greatly improved our knowledge on the role of fluids in fault zones. A part of this study was founded by the ACI "Risques Naturels" and ACI "Jeunes Chercheurs" and the computations presented in this paper were performed at the Service Commun de Calcul Intensif de l'Observatoire de Grenoble (SCCI). A.C. thanks ASSEDIC for its support.

## References

Anderson, J., J. Brune, J. Louie, Y. Zheng, M. Savage, G. Yu, Q. Chen, and D. dePolo, Seismicity in the western Great Basin apparently triggered by the Landers, California, earthquake, 28 June 1992, *Bull. Seismol. Soc. Am.*, *84*, 863–891, 1994.

Beeler, N. M., and D. A. Lockner, Why earthquakes correlate weakly with Earth tides: The effects of periodic stress on the rate and probability of earthquake occurrence, *J. Geophys. Res.*, *108*, doi:10.1029/2001JB001518, in press, 2003.

Belardinelli, M. E., M. Cocco, O. Coutant, and F. Cotton, Redistribution of dynamic stress during coseismic ruptures: Evidence for fault interaction and earthquake triggering, *J. Geophys. Res.*, *104*, 14,925–14,946, 1999.

Blanpied, M. L., D. A. Lockner, and J. D. Byerlee, Fault stability inferred from granite sliding experiments at hydrothermal conditions, *Geophys. Res. Lett.*, *18*(4), 609–612, 1991.

Brodsky, E. E., V. Karakostas, and H. Kanamori, A new observation of dynamically triggered regional seismicity: Earthquakes in Greece following the August, 1999 Izmit, Turkey earthquake, *Geophys. Res. Lett.*, *27*, 2741–2744, 2000.

Dieterich, J. H., Modeling of rock friction, 1, Experimental results and constitutive equations, *J. Geophys. Res.*, *84*, 2161–2168, 1979.

Dieterich, J. H., Earthquake nucleation on faults with rate- and state-dependent strength, *Tectonophysics*, *211*, 115–134, 1992.

Dieterich, J. H., A constitutive law for rate of earthquake production and its application to earthquake clustering, *J. Geophys. Res.*, *99*, 2601–2618, 1994.

Gomberg, J., and P. Bodin, Triggering of the Little Skull Mountain Nevada earthquake with dynamic strains, *Bull. Seismol. Soc. Am.*, *84*, 844–853, 1994.

Gomberg, J., and S. Davis, Stress/strain changes and triggered seismicity at The Geysers, California, *J. Geophys. Res.*, *101*, 733–750, 1996.

Gomberg, J., M. Blanpied, and N. Beeler, Transient triggering of near and distant earthquakes, *Bull. Seismol. Soc. Am.*, *87*, 294–309, 1997.

Gomberg, J., N. M. Beeler, M. L. Blanpied, and P. Bodin, Earthquake triggering by transient and static deformations, *J. Geophys. Res.*, *103*, 24,411–24,426, 1998.

Gomberg, J., P. A. Reasenberg, P. Bodin, and R. H. Harris, Earthquake triggering by seismic waves following the Landers and Hector Mine earthquake, *Nature*, *411*, 462–466, 2001.

Harris, R. A., Introduction to special section: Stress triggers, stress shadows, and implications for seismic hazard, *J. Geophys. Res.*, *103*, 24,347–24,358, 1998.

Linker, M. F., and J. H. Dieterich, Effects of variable normal stress on rock friction: Observations and constitutive equations, *J. Geophys. Res.*, *97*, 4923–4940, 1992.

Lockner, D. A., and N. M. Beeler, Premonitory slip and tidal triggering of earthquakes, *J. Geophys. Res.*, *104*, 20,133–20,151, 1999.

Marone, C., Laboratory-derived friction laws and their application to seismic faulting, *Annu. Rev. Eath Planet. Sci.*, *26*, 643–696, 1998.

Perfettini, H., and J. Schmittbuhl, Periodic loading on a creeping fault: Implications for tides, *Geophys. Res. Lett.*, *28*, 435–438, 2001.

Perfettini, H., J. Schmittbuhl, and A. Cochard, Shear and normal load perturbations on a two-dimensional continuous fault: 1. Static triggering, *J. Geophys. Res.*, *108*, doi:10.1029/2002JB001804, in press, 2003.

Press, W. H., B. P. Flannery, S. A. Teukolsky, and W. T. Vetterling, Integration of ordinary differential equations, in *Numerical Recipes in C, The Art of Scientific Computing*, 2nd ed., pp. 707–752, Cambridge Univ. Press, New York, 1992.

Rice, J. R., Spatio-temporal complexity of slip on a fault, *J. Geophys. Res.*, *98*, 9885–9907, 1993.

Richardson, E., and C. J. Marone, Effects of normal stress vibrations on frictional healing, *J. Geophys. Res.*, *104*, 28,859–28,878, 1999.

Roy, M., and C. Marone, Earthquake nucleation on model faults with rate - and state-dependent friction: Effects of inertia, *J. Geophys. Res.*, *101*, 13,919–13,932, 1996.

Ruina, A. L., Slip instability and state variable friction laws, *J. Geophys. Res.*, *88*, 10,359–10,370, 1983.

Stuart, W. D., and T. E. Tullis, Fault model for preseismic deformation at Parkfield, California, *J. Geophys. Res.*, *100*, 24,079–24,099, 1995.

Toda, S., R. S. Stein, P. A. Reasenberg, and J. H. Dieterich, Stress transferred by the $M_w$ = 6.9 Kobe, Japan, shock: Effect on aftershocks and future earthquake probabilities, *J. Geophys. Res.*, *103*, 24,543–24,565, 1998.

Tsuruoka, H., M. Ohtake, and H. Sato, Statistical test of the tidal triggering of earthquakes: Contribution of the ocean tide loading effect, *Geophys. J. Int.*, *122*, 183–194, 1995.

Vidale, J. E., D. C. Agnew, M. J. S. Johnston, and D. H. Oppenheimer, Absence of earthquake correlation with Earth tides: An indication of high preseimic fault stress rate, *J. Geophys. Res.*, *103*, 24,567–24,572, 1998.

Voisin, C., Dynamic triggering of earthquakes: The linear slip-dependent friction case, *Geophys. Res. Lett.*, *28*, 3357–3360, 2001.

A. Cochard, 14, rue Fagon, F-75013 Paris, France. (cochard@esag.harvard.edu)

H. Perfettini, Laboratoire de Géophysique Interne et Tectonophysique, BP 53X, F-38041 Grenoble Cedex, France. (hugo.perfettini@obs.ujf-grenoble.fr)

J. Schmittbuhl, Laboratoire de Géologie UMR 8538, Ecole Normale Supérieure, 24, rue Lhomond, F-75231 Paris cedex 05, France. (jean.schmittbuhl@ens.fr)